

Spectroelectrochemistry of Electrogenenerated Tetrathiafulvalene-Derivatized Poly(thiophenes): Toward a Rational Design of Organic Conductors with Mixed Conduction

Laurent Huchet, Said Akoudad, Eric Levillain, and Jean Roncali^{*,†}

Ingénierie Moléculaire et Matériaux Organiques, CNRS UMR 6501, Université d'Angers, 2 Bd Lavoisier, F-49045 Angers, France

Andreas Emge and Peter Bäuerle

Abteilung Organische Chemie II, Universität Ulm, Albert-Einstein-Allee 11 D-89081 Ulm, Germany

Received: June 11, 1998

Thin films of tetrathiafulvalene (TTF) derivatized polythiophenes were prepared by electropolymerization of precursors based on bithiophene or hybrid thiophene–ethylenedioxythiophene (EDOT). The cyclic voltammogram of these polymers exhibits an additional anodic wave between the two oxidation steps corresponding to the formation of the TTF cation radical and dication. The electrochemically induced spectral changes associated with these various oxidation processes were analyzed on equilibrated films and in dynamic conditions using classical and time-resolved spectroelectrochemical techniques. In spite of a complex behavior due to the overlap of the various TTF oxidations with the doping process of the π -conjugated supporting PT backbone, the different monomeric and dimeric oxidized TTF species present in the polymers were unequivocally identified. Comparison of the two polymers shows that whereas for poly(1) oxidation of TTF precedes the PT doping, the presence of EDOT in the PT backbone of poly(2) leads to the reverse situation. On the basis of these results, the structural conditions required to develop a novel class of organic conductors with mixed conduction are discussed.

Cation radical salts of tetrathiafulvalene (TTF) represent an important class of molecular conducting materials intensively investigated for more than two decades on the basis of the low-temperature superconductivity exhibited by some of the members.¹ Whereas incorporation of TTF into polymeric matrixes in view of improving the processability of TTF-based conductors was investigated several years ago,^{2,3} the association of TTF with linear π -conjugated structures is a relatively recent concept.⁴ The grafting of a TTF moiety onto an electropolymerizable monomer was initially developed by Bryce et al. as a possible strategy to indirectly control the long-range order of electrogenerated poly(thiophene) (PT) thanks to the strong propensity of TTF to self-assemble into regular π -stacks.⁵ While such hybrid materials can also contribute to a large increase of the charge storage capacity of PT, an exciting long-term prospect involves the possible development of a novel class of organic conductors in which the overall electrical conductivity would be ensured by two parallel charge-transport mechanisms, namely the intrastack aromaticity transfer associated with the mixed-valence interactions in TTF π -stacks⁶ and the polaron/bipolaron conduction in the π -conjugated chain.⁷ In addition to eventual synergistic effects, such a combination may contribute to increase the dimensionality of the conduction process.

However, the design of precursors capable to lead to such materials poses considerable problems. As a matter of fact, the structure of the precursor must simultaneously fulfill multiple stringent prerequisites such as (i) neutralization of the eventual electronic and/or steric effects of the attached TTF group on the electropolymerization reaction and on the effective conjuga-

tion of the resulting polymer, (ii) adequate packing arrangement of the TTF groups in the polymer allowing mixed-valence interactions and hence intrastack conduction, and (iii) precise tuning of the oxidation potential of both the TTF group and the π -conjugated support in order that both components of the system possess a common potential window of conductivity.

A first attempt to electropolymerize TTF-derivatized thiophene monomers was reported in 1990.⁵ Following this seminal work, different thiophenic precursors have been synthesized.^{8–10} Although unequivocal evidence for electropolymerization was reported in one case,⁸ the large potential difference between the first TTF oxidation (ca. 0.40 V/SCE) and the potential needed to polymerize the substituted thiophene (1.80 V) was identified as a serious problem.⁸ Recently, we have shown that thanks to a much lower electropolymerization potential, TTF-substituted bithiophenic precursors are readily converted into extensively π -conjugated TTF-derivatized poly(thiophenes) with interesting electrochemical properties.¹¹ In particular, the cyclic voltammogram (CV) of these polymers has revealed an hitherto unknown additional oxidation wave at a potential intermediate between those corresponding to the generation of the TTF cation radical and dication.¹¹

In this work, the different redox steps involved in the overall doping process of these polymers have been analyzed on equilibrated films and in dynamic conditions using classical and time-resolved spectroelectrochemical techniques. The various monomeric and dimeric oxidized TTF species occurring in the polymer as a function of the electrode potential have been identified while the major role of the conjugated PT support has been evidenced by the use of two polymer structures ((poly-

[†] E-mail: jean.roncali@univ-angers.fr.

CHART 1

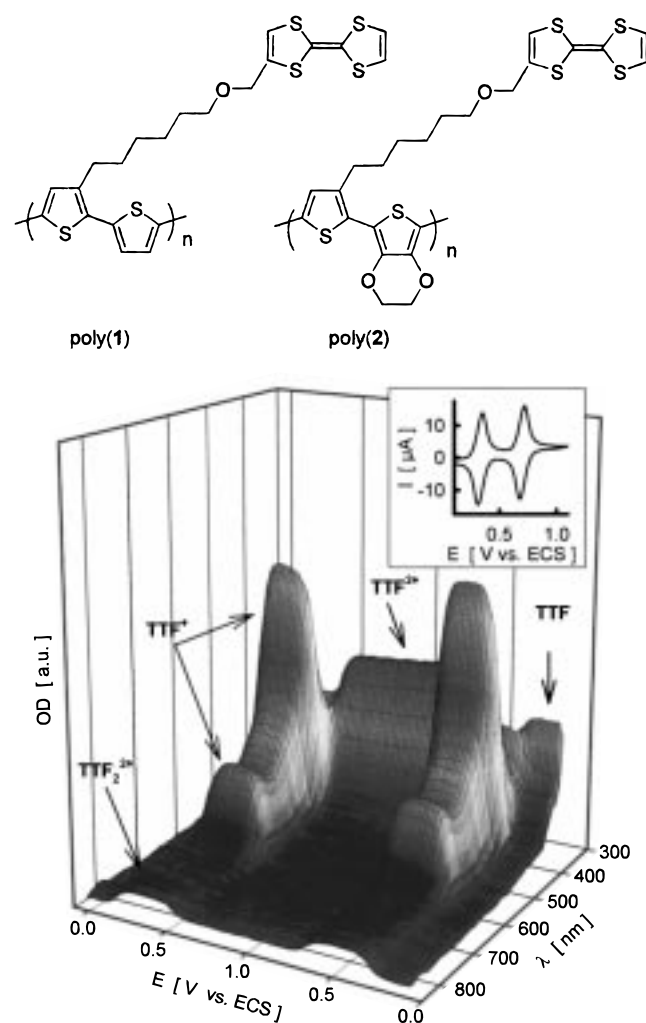


Figure 1. Spectroelectrochemistry of TTF (ca. 5 mM) under thin layer diffusion conditions ($d \approx 25 \mu\text{m}$) in 10^{-1} M TBAHP/ CH_3CN , reference SCE, scan rate 2 mV s^{-1} .

(1) and poly(2) (Chart 1)), which differ by the onset potential for doping and hence by the potential window of conductivity. These various results are discussed in the more general context of the structural conditions required to design possible precursors of an organic material with hybrid conduction.

Results

Although TTF derivatives have been investigated for years in the general frame of organic metals,¹ data concerning the spectral signature of the various oxidized forms and in particular the dication remain scarce and not always devoid of ambiguity. Therefore, prior to analyzing the spectroelectrochemistry of the polymers, the behavior of TTF has been analyzed in the 300–900 nm spectral range by time-resolved spectroelectrochemistry. Figure 1 shows the potential dependence of the electronic absorption spectrum of TTF in acetonitrile during a 2 mV s^{-1} voltammetric cycle. Oxidation leads to the rapid disappearance of TTF absorption at 320 nm and to the development of two new bands with maxima at 430 and 580 nm characteristic for the cation radical $\text{TTF}^{\bullet+}$.¹² In the same potential region a weak absorption band emerges around 800 nm which can be assigned to the π -dimer $(\text{TTF})_2^{2+}$.¹² Beyond 0.70 V the spectrum shows only a single absorption band with a λ_{max} at 390 nm which can be unequivocally assigned to the dication TTF^{2+} .

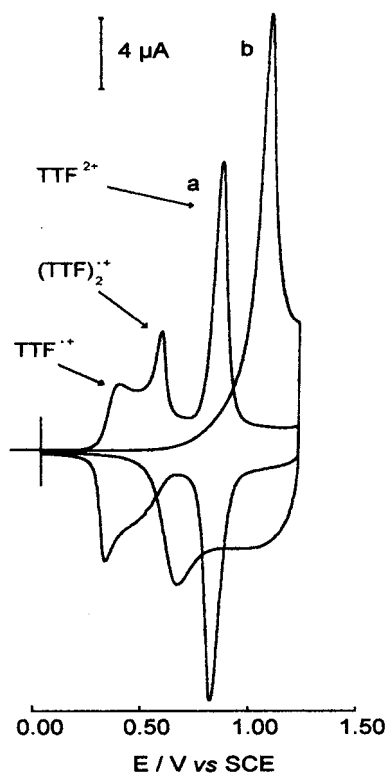


Figure 2. Cyclic voltammograms recorded in 10^{-1} M $\text{Bu}_4\text{NPF}_6/\text{CH}_3\text{CN}$, scan rate 100 mV s^{-1} : (a) poly(1), (b) poly(BT).

In their pioneering work on TTF-derivatized polystyrene films, Chambers et al. attributed the main absorption band of the cation radical to a band at 393 nm and that of the dication to a band at 533 nm.^{3a} As suggested by the results below, these wavelengths might correspond in fact to intramolecular transitions of the π -dimer $(\text{TTF})_2^{2+}$ for which a rather large potential window of existence is found.

Figure 2 shows the superposition of the CV of poly(1) and poly(bithiophene) (PBT) recorded in the same conditions (the CV of poly(2) is very similar to that of poly(1)).¹¹ The fact that the response of the PBT backbone is not observed in the CV of the polymers can be related to the much larger amount of charge involved in TTF oxidation (2 electrons/TTF vs 0.10–0.20 electron/thiophene for PBT).¹³

In previous works on TTF-derivatized polystyrene³ or PT,⁸ a broadening of the first reduction wave of TTF was observed and attributed to the overlap of the reduction of $\text{TTF}^{\bullet+}$ and its π -dimer $(\text{TTF})_2^{2+}$ with that of the mixed-valence (MV) dimer $(\text{TTF})_2^{\bullet+}$. As shown in Figure 2, instead of a simple wave broadening, the CV of poly(1) and poly(2) exhibits an additional well-defined anodic wave between the two TTF oxidation steps. The aggregate origin of this hitherto unknown new oxidation steps was previously established by its progressive disappearance when 1 was incorporated in the backbone of copolymers containing increasing amounts of unsubstituted BT.¹¹

Figure 3, a and b, show the in situ electronic absorption spectra of poly(1) at various applied potentials. The spectrum recorded at -0.40 V shows the absorption band of neutral TTF (TTF_0) with λ_{max} at 320 nm and a broad band with λ_{max} at 500 nm corresponding to the absorption of the neutral PBT backbone (PBT_0).^{13,14} Increasing the applied potential up to ca. $+0.65 \text{ V}$ leaves the absorbance at 500 nm practically unchanged. In agreement with the CV of PBT (Figure 2), this result implies that hole injection in the PBT backbone starts only beyond this potential. Consequently, all optical changes observed in the

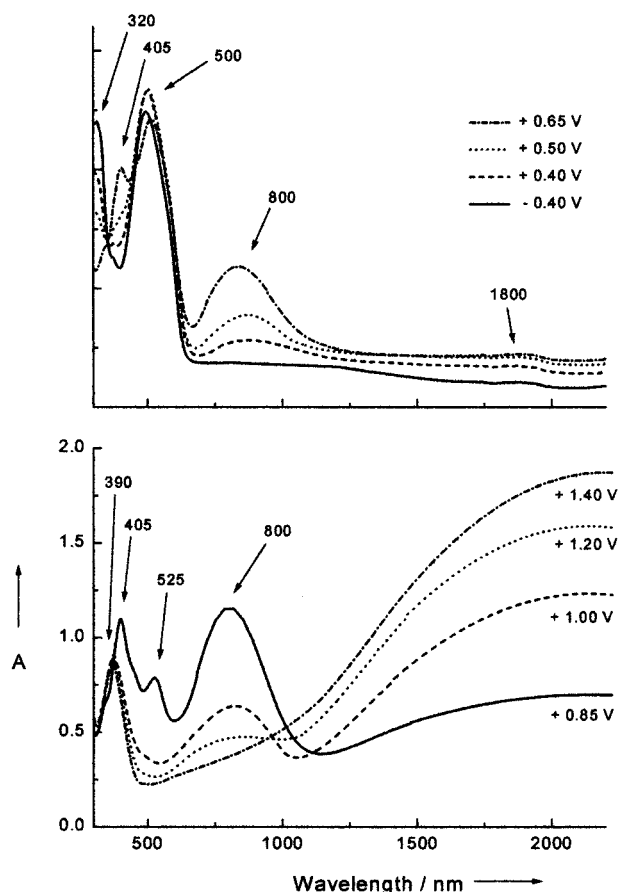


Figure 3. In situ electronic absorption spectra of poly(1) at various applied potentials. Electrolytic medium 10^{-1} M TBAHP/ CH_3CN , reference Ag^+/AgCl .

-0.40 to $+0.65$ V potential window (Figure 3a) can be unequivocally assigned to the TTF electrochemistry. The increase of the applied potential in this range produces a progressive decrease of the TTF_0 absorption at 320 nm and the parallel emergence of a new band at 800 nm. This band, which corresponds the intermolecular charge-transfer (CT) band of the π -dimer $(\text{TTF})_2^{2+}$,¹² has already been observed for TTF-derivatized polystyrene.³ This π -dimer is expected to show two intramolecular transitions at ca. 390 and 515 nm.¹² While the latter cannot be observed due to the overlap with the PBT_0 absorption, the former can be assigned to the peak emerging at 405 nm. On the other hand, the spectra recorded between $+0.40$ and $+0.65$ V reveal the parallel emergence of a band of weak intensity in the 1800 nm region. This band, which corresponds to an intermolecular transition of the mixed valence (MV) TTF dimer $(\text{TTF})_2^{\bullet+}$, can be viewed as an anticipation of the optical conduction band observed in the reflectance spectrum of metallic TTF cation radical salts.¹² This band appears more clearly in the spectrum obtained by subtracting the -0.40 V spectrum of the $+0.40$ V (Figure 4). This spectrum also exhibits the two intramolecular transitions of the π -dimer $(\text{TTF})_2^{2+}$ at 400 and 525 nm and the intermolecular CT band at 800 nm. Another peak is observed at 600 nm which may be assigned to the unaggregate cation radical $\text{TTF}^{\bullet+}$. Thus, this spectrum corresponds to a rather unique situation in which the neutral TTF, the free cation radical, the MV dimer, and the π -dimer are simultaneously present in the film.

Application of potentials positive of $+0.65$ V triggers the doping of the PT backbone as shown by the decrease of the PT_0 absorption at 500 nm (Figure 3b). Concurrently, a red shift of λ_{max} from 500 to 530 nm occurs. As shown in Figure 4, this

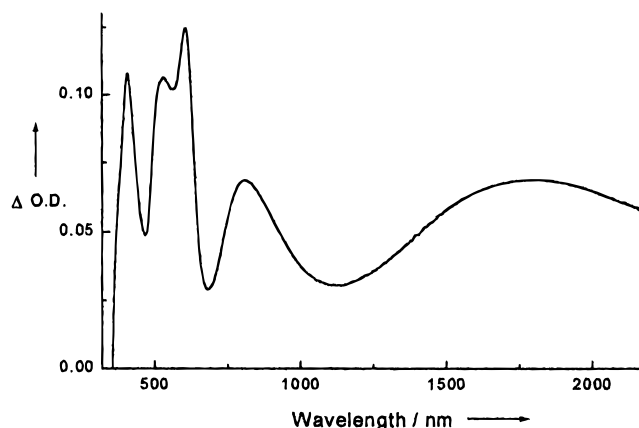


Figure 4. Difference spectrum between the spectra recorded at $+0.40$ V and -0.40 V in Figure 3a.

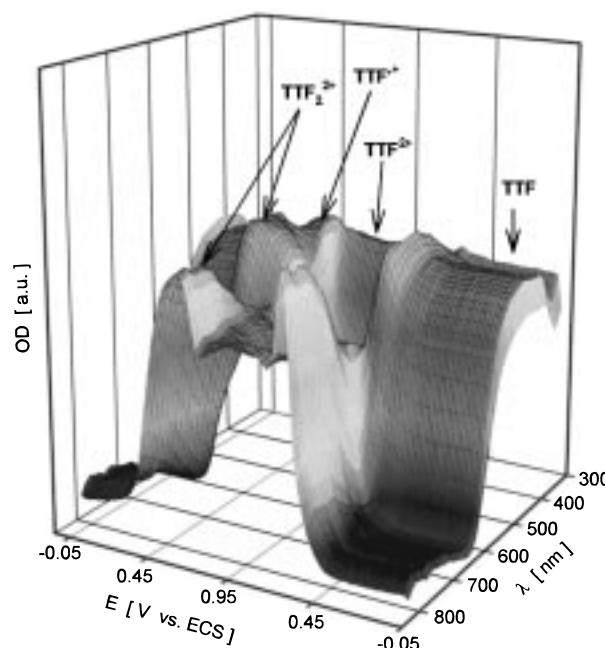


Figure 5. Spectroelectrochemistry of poly(1) in 10^{-1} M TBAHP/ CH_3CN , reference SCE, scan rate 1 mV s^{-1} .

apparent shift results in fact from the disappearance of PBT_0 which puts in evidence the second intramolecular transition of $(\text{TTF})_2^{2+}$ at 525 nm. As expected, the decrease of the PBT_0 absorption at 500 nm is accompanied by the emergence of two bipolaronic transitions around 800 and 2000 nm.¹⁴ The unusually high relative intensity of the 800 nm band is due to an overlap with the intermolecular CT band of $(\text{TTF})_2^{2+}$. At an applied potential of 0.85 V, formation of TTF^{2+} starts, and between $+0.85$ and $+1.40$ V the intensity of the $(\text{TTF})_2^{2+}$ intra- and intermolecular transitions at 405, 530, and 800 nm, respectively, decreases while the spectrum of the PBT backbone turns to the characteristic free-carrier absorption of the metallic state.^{14,15} The fact that the 390 nm band is the only surviving spectral signature of TTF definitively confirms its assignment to TTF^{2+} .

The time-resolved spectroelectrochemical response in Figure 5 summarizes the spectral changes associated with the interconversion of the various TTF species during a complete voltammetric scan. The intra- and intermolecular transitions of the π -dimer are observed at the potential corresponding to the onset of TTF oxidation while conversion of the π -dimer into the dication occurs at the potential of the second anodic peak of TTF. Contrary to Figure 1, the spectra obtained during

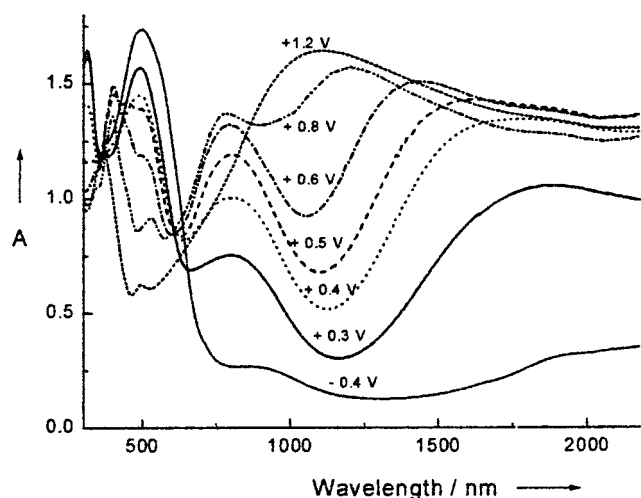


Figure 6. In situ electronic absorption spectra of poly(2) at various applied potentials. Electrolytic medium same as for Figure 2.

the forward and backward scan are not identical. Thus, in the beginning of the reverse scan a weak absorption band emerges at ca. 430 nm which corresponds to the main absorption band of the cation radical (see Figure 1). This suggests that the dication is first reduced into the free cation radical which, shortly after, dimerizes into the π -dimer whose spectral signature reinforces when the potential reaches the 0.90–0.80 V range.

The spectroelectrochemical analysis of poly(2) is shown in Figure 6. After more than 40 min at -0.40 V the spectrum still exhibits weak residual absorption around 800–1000 nm and 1800–2000 nm which illustrates the difficulty to fully undope the polymer.¹¹ On the basis of the high stability of doped poly(EDOT),¹⁶ this effect can be related to the incorporation of EDOT in the PT backbone. The -0.40 V spectrum shows the TTF_0 band at 320 nm and the broad PT_0 absorption with a maximum at 512 nm. The absorption edge at 730 nm (1.70 eV) confirms, as expected, that the presence of EDOT in the π -conjugated backbone decreases the band gap to a value intermediate between that of poly(EDOT) (1.65 eV)¹⁷ and poly(BT) (2.00 eV).^{13,14}

Increasing the applied potential up to $+0.40$ V does not affect the TTF_0 absorption but produces a slight decrease of the absorption of the PT backbone and a related increase of the bipolaronic transitions around 800 and 2000 nm. This significant decrease of the onset potential for doping compared to poly(1) is due again to the presence of EDOT in the structure. These results show that the very similar CVs of the two polymers correspond in fact to two different situations. As for poly(1), oxidation of TTF starts at $+0.40$ V as shown by the decrease of the TTF_0 band at 320 nm. Contrary to poly(1), the absorption of the MV dimer $(\text{TTF})_2^{2+}$ around 1800 nm cannot be observed due to the overlap with PT backbone absorption. The $+0.50$ V spectrum shows the PT_0 band at 510 nm and two peaks at 405 and 435 nm corresponding to $(\text{TTF})_2^{2+}$ and TTF^+ respectively. In addition, the long-wavelength bipolaron band shifts hypsochromically to 1600 nm. The spectra recorded at $+0.60$ and $+0.80$ V are dominated by the intra- and intermolecular transitions of the π -dimer $(\text{TTF})_2^{2+}$ at 405 and 800 nm, respectively, with a further blue shift of the low-energy band to 1200 nm. Finally, at the highest potential (1.00 V), the only remaining spectral signature of TTF is again the 380 nm dication band while the two PT bipolaron bands merge into a single broad band with a maximum around 1150 nm.

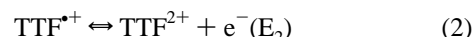
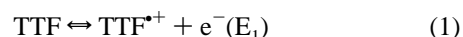
Comparison of the spectra of the two polymers at the highest doping level shows that while the spectrum of poly(1) is typical

for doped PT,^{13–15} the behavior of poly(2) is more reminiscent of that of isolated thiophene oligomers in solution. In this case, the two transitions of the cation radical (polaron model) are progressively replaced by a single transition at intermediate energy upon oxidation to the dication.¹⁸ While the unusual spectrum of doped poly(2) is clearly due to the presence of EDOT in the PT backbone, the interpretation of this behavior is not straightforward. A similar phenomenon has already been observed for polymers prepared from asymmetric bithiophenes and attributed to the confinement of charge carriers.¹⁹ Another possibility may involve a weakening of interchain interactions caused by intermolecular Coulombic repulsion between localized positive charges. Such an interpretation would imply that the near-IR band of poly(1) corresponds to the optical conduction band related to a π -stacking of PT chains according to the interpretation proposed by Miller et al.²⁰ Further work is clearly needed to clarify this question.

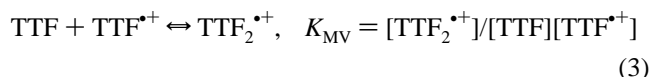
Discussion

These various spectroelectrochemical experiments clearly show that the conversion of the attached TTF into its dication involves in fact the transient formation of aggregate species which are not or hardly observed in dilute solution. These results allow to reexamine the redox processes in the film from a different viewpoint.

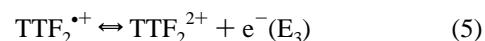
The solution CV of TTF (Figure 1) shows two reversible steps according to



The first oxidation step can be eventually followed by formation of a MV dimer and/or a π -dimer:



The full reversibility of the first and second oxidation steps shows that they are not under kinetic control. On the other hand, since $\text{TTF}_2^{\bullet+}$ and TTF_2^{2+} are conjugated species of the same redox couple.



The corresponding redox potential (E_3) is thus related to E_1 , K_{MV} , and $K_{\pi\text{-Dim}}$ by

$$E_3 = E_1 + RT/F \ln [K_{\text{MV}}/K_{\pi\text{-Dim}}] \quad (6)$$

Since E_3 is greater than E_1 it follows that, $K_{\text{MV}} > K_{\pi\text{-Dim}}$. Unlike the solution CV, that of the polymers exhibits an additional anodic wave after the first oxidation step. As shown by spectroelectrochemical experiments, while the MV dimer is formed during the first oxidation step (E_1), the π -dimer results from the oxidation of the MV dimer in the second step (E_3) and the dication is formed during the last step (E_2). After initial oxidation of TTF into $\text{TTF}^{\bullet+}$ at E_1 , rapid formation of the MV dimer by reaction of $\text{TTF}^{\bullet+}$ with TTF_0 occurs (eq 3). This dimerization leads to the consumption of TTF_0 which explains the limited intensity of the first anodic wave in Figure 2 compared to Figure 1. Similarly, the occurrence of an additional

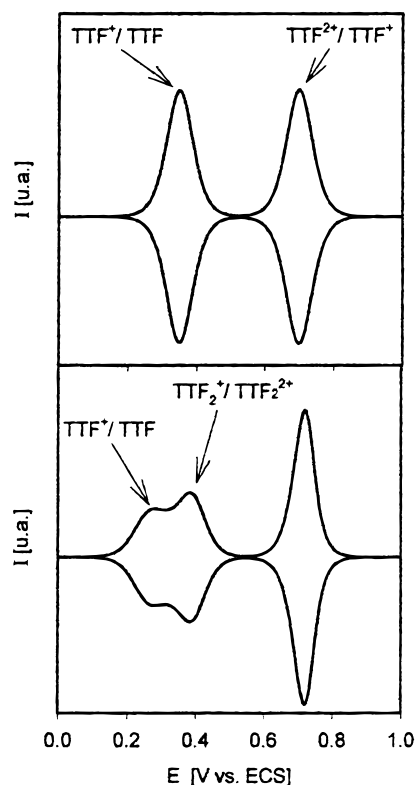


Figure 7. Simulated cyclic voltammograms (Digisim 2.1) in thin layer conditions ($1 \mu\text{m}$ and 1 mV s^{-1}). Simulation was carried out with the same set of parameters for two substrate concentrations (1 mM (top) and 1 M (bottom)). Redox potentials: $E_1 = 0.35 \text{ V}$; $E_3 = 0.40 \text{ V}$; $E_2 = 0.70 \text{ V}$. Charge-transfer parameters: $k = 1 \text{ cm s}^{-1}$, $\alpha = 0.5$, $D = 10^{-6} \text{ cm}^2 \text{ s}^{-1}$. Chemical reaction parameters: $K_{\text{MV}} = 14.5 \text{ M}^{-1}$, $k_{\text{MV}} = 100 \text{ M}^{-1} \text{ s}^{-1}$ and $K_{\pi\text{-Dim}} = 2 \text{ M}^{-1}$, $k_{\pi\text{-Dim}} = 100 \text{ M}^{-1} \text{ s}^{-1}$. $T = 298 \text{ K}$. E_3 and E_1 are related by eq 5 and there is no kinetic limitation at this scan rate.

oxidation step at E_3 (eq 5) instead of the simple wave broadening observed in previous works can be explained by the presence of much larger amounts of MV dimer. This high concentration of MV dimer subsequently converted into π -dimer can account for the fact that the free cation radical is hardly detected during the whole oxidation process. Thus, beyond E_3 the film contains essentially the π -dimer and oxidation of $\text{TTF}^{\bullet+}$ into TTF^{2+} is observed without delay because of the fast dissociation of $(\text{TTF})_2^{2+}$ into $\text{TTF}^{\bullet+}$ relative to scan rate.

Figure 7 shows the CV simulated in thin layer conditions for a dilute ($C = 1 \text{ mM}$) and a concentrated solution ($C = 1 \text{ M}$) taken as a representation for the film situation. Comparison with experiment shows qualitatively good agreement even if simulation does not take into account the potential dependence of the film conductivity and its consequences for the various charge-transfer processes. With this provision in mind, this result seems to indicate that the much higher TTF concentration present in the polymer is in favor of the π -dimer formation to the detriment of that of the MV dimer (eq 4).

It is well-known that the appearance of metallic conductivity in cations radical salts of TTF requires the development of intrastack MV interactions while, in contrast, materials with an integer valence are in general insulating.^{1,21} As shown by Torrance et al., the MV dimer and the π -dimer represent the solution counterpart of these two situations and these aggregate species can thus be viewed as models that anticipate the final stoichiometry of the material.¹²

The above results provide conclusive evidence for the occurrence of large amounts of MV dimer and π -dimer in our

polymers. While this self-organization among attached TTF groups already represents an interesting result, at the potential needed to electropolymerize the attached BT precursor, initially formed MV dimers are successively converted into π -dimers and dications. Consequently, MV interactions must be reconstructed by subsequent undoping and controlled reoxidation of the polymer and this process can be expected to result in a partial loss of the initial order. While the tuning of the potential window of conductivity of the PT support achieved in poly(2) already represents an interesting step, simultaneous formation of a MV TTF cation radical salt and doped PT support during a single-step electrodeposition process would represent a considerable progress toward the synthesis of a polymer with hybrid conduction. Such an objective implies filling the gap between the first oxidation potential of the attached TTF and the electropolymerization potential. In this context, future precursor design could resort to three possible strategies, namely (i) a further decrease of the electropolymerization potential, in this regard the recently synthesized EDOT dimer²² and trimer²³ could represent interesting building blocks, (ii) an increase of the first oxidation potential of the attached TTF by electron-withdrawing substituents (introduction of an ethylenedithio group appearing particularly attractive), and (iii) an increase of TTF concentration in the polymer by grafting more than one TTF unit on the precursor structure. Work along these lines is now in progress in our laboratory and will be reported in the near future.

Experimental Section

The precursors 3-[7-oxa-8-(2-tetrathiafulvalenyl)octyl]-2,2'-bithiophene (**1**) and 3-[7-oxa-8-(2-tetrathiafulvalenyl)octyl]-3',4'-ethylenedioxy]-2,2'-bithiophene (**2**) were synthesized according to the previously reported procedures.¹¹

Electrochemical experiments were carried out with a PAR 273 potentiostat-galvanostat. Cyclic voltammetry was performed in a three-electrode single-compartment cell equipped with platinum microelectrodes of $7.85 \times 10^{-3} \text{ cm}^2$ area, a platinum wire counter-electrode, and a saturated calomel reference electrode (SCE). Films for CV were deposited on Pt microelectrodes in potentiostatic conditions at the foot of the oxidation peak, namely 1.30 and 1.15 V/SCE for **1** and **2**, respectively. The electrolytic medium involved $2 \times 10^{-2} \text{ M}$ of precursor and 0.10 M of tetrabutylammonium hexafluorophosphate (TBAHP) (Fluka puriss) in nitrobenzene. Cyclic voltammetry was performed in acetonitrile solutions (HPLC grade) containing 0.10 M TBAHP. All solutions were deaerated by argon bubbling prior to each experiment which was run under inert atmosphere. Films for spectroelectrochemistry were grown on a Pt electrode of 0.5 cm diameter by application of recurrent potential scans (100 mV s^{-1}) between 0.0 V and the above indicated positive potentials. Spectroelectrochemical experiments were performed in a thin-layer cell containing 0.20 M TBAHP in MeCN. A Pt ring served as counter electrode and Ag/AgCl wire as reference. The initial spectrum of the undoped polymer was recorded once again at the end of each set of experiments in order to rule out a possible degradation of the polymer in the course of the experiments. Time-resolved spectroelectrochemistry was performed using the already described experimental setup.²⁴

References and Notes

- (1) Williams, J. M.; Ferraro, J. R.; Thorn, R. J.; Carlson, K. D.; Geiser, U.; Wang, H. H.; Kini, A. M.; Whangbo, M. H. *Organic Superconductors (Including Fullerenes)*; Prentice-Hall: Englewood Cliffs, NJ, 1992. Bryce,

M. R. *Chem. Soc. Rev.* **1991**, 20, 355. Schukat, G.; Fanghänel, E. *Sulfur Rep.* **1996**, 18, 1.

(2) (a) Hertler W. R. *J. Org. Chem.* **1975**, 41, 1412. (b) Pittman, Jr, C. U.; Narita, M.; Liang, Y.F. *Macromolecules* **1976**, 9, 359. (c) Pittman, Jr, C. U.; Liang, Y. F. Narita, M.; Ueda, M. *Macromolecules* **1979**, 12, 541. (d) Hinh, L. Schukat, G.; Fanghänel, E. *J. Prakt. Chem.* **1979**, 321, 299. (e) Kossmehl, G.; Rohde, M. *Makromol. Chem.* **1982**, 183, 2077. (f) Henning, T. P.; White, H. S.; Bard, A. J. *J. Am. Chem. Soc.* **1981**, 103, 3937.

(3) (a) Kaufman, F. B.; Shroeder, A. H.; Engler, E. M.; Kramer, S. R.; Chambers, J. P. *J. Am. Chem. Soc.* **1980**, 102, 483. (b) Chambers, J. Q.; Kaufman, F. B.; Nichols, K. H. *J. Electroanal. Chem.* **1982**, 142, 277. (c) Inzelt, G.; Chambers, J. Q.; Kaufman, F. B. *J. Electroanal. Chem.* **1983**, 159, 443.

(4) (a) Adam, M.; Müllen, K. *Adv. Mater.* **1994**, 6, 439. (b) Bryce, M. R. *J. Mater. Chem.* **1995**, 5, 1481. (c) Roncali, J. *J. Mater. Chem.* **1997**, 7, 2307.

(5) Bryce, M. R.; Chissel, A. D.; Gopal, J.; Kathirgamanathan, P.; Parker, D. *Synth. Met.* **1991**, 39, 397.

(6) Perlstein, J. H. *Angew. Chem., Int. Ed. Engl.* **1977**, 16, 519.

(7) (a) Brédas, J. L.; Thémans, B.; André, J. M.; Chance, R. R. Chance, Silbey, R. *Synth. Met.* **1984**, 9, 265. (b) Heeger, A. J.; Kivelson, S.; Schrieffer, J. R.; Su, W.-P. *Rev. Mod. Phys.* **1988**, 781, 60.

(8) Thobie-Gautier, C.; Gorgues, A.; Jubault, M.; Roncali, J. *Macromolecules* **1993**, 6, 4094.

(9) (a) Charlton, A.; Underhill, A. E.; Williams, G.; Kalaji, M.; Murphy, P. J.; Hibbs, D. E.; Hursthouse, M. B.; Abdul Malik, K. M. *Chem. Commun.* **1996**, 2423. (b) Charlton, A.; Underhill, A. E.; Williams, G.; Kalaji, M.;

Murphy, P. J.; Abdul Malik, K. M.; Hursthouse, M. B. *J. Org. Chem.* **1997**, 62, 3098.

(10) Skabara, P. J.; Müllen, K. *Synth. Met.* **1997**, 84, 345.

(11) Huchet, L.; Akoudad, S.; Roncali, J. *Adv. Mater.* **1998**, 10, 541.

(12) Torrance, J. B.; Scott, B. A.; Welber, B.; Kaufman, F. B.; Seiden, P. E. *Phys. Rev. B* **1979**, 19, 730.

(13) Roncali, J. *Chem. Rev.* **1992**, 92, 711.

(14) Patil, A. O.; Heeger, A. J.; Wudl, F. *Chem. Rev.* **1988**, 88, 183.

(15) Roncali, J.; Marque, P.; Garreau, R.; Yassar, A.; Garnier, F.; Lemaire, M. *Macromolecules* **1990**, 23, 1347.

(16) Jonas, F.; Morrison, J. T. *Synth. Met.* **1997**, 85, 1397.

(17) Dietrich, M.; Heinze, J.; Heywang, G.; Jonas, F. *J. Electroanal. Chem.* **1994**, 369, 87.

(18) (a) Caspar, J. V.; Ramamurthy, V.; Corbin, D. R. *J. Am. Chem. Soc.* **1991**, 113, 600. (b) Guay, J.; Kasai, P.; Diaz, A.; Wu, R.; Tour, J. M.; Dao, L. H. *Chem. Mater.* **1992**, 4, 1097. (c) P. Bäuerle, U. Segelbacher, K.-U. Gaudl, Huttenlocher, D.; Mehring, M. *Angew. Chem., Int. Ed. Engl.* **1993**, 32, 76.

(19) (a) Faïd, K.; Leclerc, M.; Nguyen, M.; Diaz, A. *Macromolecules* **1995**, 28, 284. (b) Demanze, F.; Yassar, A.; Garnier, F. *Adv. Mater.* **1995**, 7, 907.

(20) Miller, L. L.; Yu, Y.; Gunic, E.; Duan, R. *Adv. Mater.* **1995**, 7, 547.

(21) Torrance, J. B. *Acc. Chem. Res.* **1979**, 12, 79.

(22) Akoudad, S.; Roncali, J. *Synth. Met.* **1998**, 93/2, 111.

(23) Sotzing, G. A.; Reynolds, J. R.; Steel, P. *Chem. Mater.* **1996**, 8, 882.

(24) Gaillard, F.; Levillain, E. *J. Electroanal. Chem.* **1995**, 398, 77.